Human modification of global water vapor flows from the land surface

Line J. Gordon*†, Will Steffen‡, Bror F. Jönsson§, Carl Folke*, Malin Falkenmark¶, and Åse Johannessen*

Departments of *Systems Ecology and §Meteorology, Stockholm University, SE-106 91 Stockholm, Sweden; ‡Bureau of Rural Sciences, Department of Agriculture, Fisheries and Forestry, Australian Government, G.P.O. Box 858, Canberra ACT 2601, Australia; and ¶Stockholm International Water Institute, Hantverkargatan 5, SE-112 21 Stockholm, Sweden

It is well documented that human modification of the hydrological cycle has profoundly affected the flow of liquid water across the Earth's land surface. Alteration of water vapor flows through land-use changes has received comparatively less attention, despite compelling evidence that such alteration can influence the functioning of the Earth System. We show that deforestation is as large a driving force as irrigation in terms of changes in the hydrological cycle. Deforestation has decreased global vapor flows from land by 4% (3,000 km³/yr), a decrease that is quantitatively as large as the increased vapor flow caused by irrigation (2,600 km³/yr). Although the net change in global vapor flows is close to zero, the spatial distributions of deforestation and irrigation are different, leading to major regional transformations of vapor-flow patterns. We analyze these changes in the light of future land-use-change projections that suggest widespread deforestation in sub-Saharan Africa and intensification of agricultural production in the Asian monsoon region. Furthermore, significant modification of vapor flows in the lands around the Indian Ocean basin will increase the risk for changes in the behavior of the Asian monsoon system. This analysis suggests that the need to increase food production in one region may affect the capability to increase food production in another. At the scale of the Earth as a whole, our results emphasize the need for climate models to take land-use change, in both land cover and irrigation, into account.

deforestation | irrigation | land-use changes | climate change | evapotranspiration

Meeting water requirements for future food production without compromising the water needs of other human life-support systems is a major challenge for future freshwater management (1, 2). Food production involves the transformation of liquid water (from irrigation or precipitation) to water vapor (evapotranspiration), and recent estimations show that annual global vapor flows from future food production are likely to double within the next 25–50 yr (3, 4). It is well known that irrigation is, by far, the largest water user in terms of liquid water withdrawal from rivers and aquifers (5, 6) and that human modification of the hydrological cycle has profoundly affected the flow of liquid water across the Earth's land surface (7–10). Alteration of water vapor flows through land-use and land-cover changes has received less attention, compared to liquid flows, although there is compelling evidence that such alterations can influence the functioning of the Earth System (11–15).

Several examples from around the world show that changes in vapor flows due to land-cover change and irrigation have affected the functioning of the terrestrial biosphere and influenced climate at local and regional scales. For example, irrigated croplands have increased vapor flows from a converted steppe in Colorado by 120% (16), contributing to higher precipitation, lower temperature, and an increase in thunderstorm activity (17, 18). Large-scale deforestation for crop- and grasslands in Australia has caused a 10% decrease in vapor flows on that continent, with consequent widespread and irreversible dryland salinity that has reduced crop productivity

in some regions and made farming impossible in others (13). Simulations of changed vapor flows due to land-cover change in East Asia have affected the behavior of the East Asian Monsoon, including a weakening of the summer monsoon low-pressure system and an increase in irregular northerly flow (12, 19). Modeled vegetation changes for agricultural expansion in West Africa have shown potentially dramatic impacts on rainfall in the African monsoon circulation, especially through deforestation along the southern coast, because this deforestation decreases the vapor flow into the region (20).

These examples, however, address only local to regional changes. No spatially explicit analysis exists of the extent of vapor-flow changes at a global scale. Here, we present a spatially explicit global estimate of changes in vapor flows as a consequence of both irrigation and deforestation. We elucidate which regions have experienced substantial changes in vapor flows as a consequence of human actions and the scale and direction of those changes. We analyze these changes and address the challenges facing future freshwater management to increase vapor flows for food production without compromising the capacity of the Earth System to support human welfare.

Methods

By comparing vapor flows from potential vegetation with flows from the actual vegetation of today, we quantify the alteration of global vapor flows due to deforestation and irrigation. Potential vegetation is here defined as the vegetation most likely to have been present in the absence of human activities, assuming a climate similar to the present one as the main determinant of biome distribution. We focused on deforestation because it has, in general, a higher impact on vapor flows than do other land-cover changes (21).

We developed a geographic information system (GIS) model of the terrestrial surface of the Earth with a spatial resolution of $0.5° \times 0.5°$. Each grid cell contains information on land cover, climate (temperature and precipitation), and percentage irrigated area. For land cover, the 5-min data set for potential vegetation (22) was regridded, by using interpolation, to 0.5° and the same land mask as the data set on actual vegetation (23). See Table 1 for the total area of the 17 vegetation types in the actual and potential vegetation datasets. Mean monthly precipitation and temperature were derived from a 30-yr (1961–1990) data set (24). The same climatic data were applied for estimating water vapor flows for both actual vegetation and potential vegetation. A digital global map of irrigated areas (25) was used to estimate the percentage of each grid that is equipped for irrigation.

Vapor-Flow Estimates

The monthly vapor flow for each vegetation type was approximated as

Table 1. Data used for the estimation of annual vapor flows from actual and potential vegetation

	Area, 10³ km²			k_{veg}	
Vegetation type	Potential vegetation	Actual vegetation	Difference, %	Summer	Winter
Intensive cropland	0	15,872*		0.30	0.60
Marginal cropland used for grazing	0			0.15	0.30
Tropical evergreen forest/woodland	19,332	16,278	−16	0.50	0.50
Tropical deciduous forest/woodland	6,153	3,062	−50	0.30	0.60
Temperate broadleaf evergreen forest/woodland	1,452	356	−75	0.50	0.50
Temperate needleleaf evergreen forest/woodland	3,591	2,134	−41	0.30	0.60
Temperate deciduous forest/woodland	6,035	2,095	−65	0.30	0.60
Boreal evergreen forest/woodland	6,608	6,356	−4	0.30	0.60
Boreal deciduous forest/woodland	3,109	2,165	−30	0.30	0.60
Evergreen deciduous mixed forest/woodland	16,260	14,222	−13	0.30	0.60
Savanna†	19,562	19,562		0.25	0.40
Grassland steppe	14,393	14,393		0.15	0.30
Dense shrubland	6,901	6,901		0.10	0.20
Open shrubland	11,748	11,748		0.15	0.25
Tundra	8,321	8,321		0.02	0.95
Hot desert	15,596	15,596		0.02	0.02
Polar desert/rock/ice	3,605	3,605		0.95	0.95
Irrigated areas‡				0.50	0.50
Total	142,657	142,667			

The data include vegetation types, areas of different vegetation types, difference in area between actual and potential vegetation, and the monthly vegetation-specific coefficient (k_{veg}).
*Area includes both intensive croplands and marginal croplands used for grazing.
†k_{veg} of savannas was originally 0.15 for summer and winter months.
‡Irrigated areas are defined as a percentage of each grid cell.

$$VF = k_{veg} \cdot PET,$$

where VF is the vapor flow, k_{veg} is the vegetation-specific coefficient (see below), and PET is the potential evapotranspiration. The PET was estimated with a modified Thornthwaite equation (26):

$$PET = 1.2 \cdot 10^9 \cdot e[-4.62 \cdot 10^3/(T + 273.15)].$$

This equation was chosen because it requires only one climatic input variable (Celsius temperature T) and because it has been suggested that Thornthwaite-based methods are as good as more refined methods when dealing with monthly data as compared with more detailed daily data (27).

A "cutoff" for precipitation was made, ensuring that the mean monthly vapor flow for each grid cell could not be larger than the mean monthly precipitation. To avoid the cutoff in irrigated lands, we estimated vapor flows from these lands separately:

$$VF_{grid} = [k_{veg} \cdot PET_{grid} \cdot (1 - irri))/100]$$
$$+ [irri(k_{veg \, irri} \cdot PET_{grid})/100],$$

where k_{veg} is the vegetation coefficient of the vegetation within that cell, $k_{veg \, irri}$ is the vegetation coefficient for irrigated crops, and $irri$ is the percentage of irrigated area within that cell.

The coefficient k_{veg} is vegetation-specific and is related to parameters that influence water uptake and transpiration, such as depth of roots, leaf area, length of growing season, and soil moisture. The k_{veg} have been developed for summer and winter values of 25 different vegetation types used in the TERRAIN subprogram of Pennsylvania State University–National Center for Atmospheric Research (PSU/NCAR) Mesoscale Model (MM5) (28); see Table 1. Monthly k_{veg} were constructed by combining the winter and summer values with weighted averaging. To account for the austral seasons, the summer and winter values of the Southern Hemisphere were switched at the equator.

For "marginal cropland/areas used for grazing" we used the same value as for natural grasslands.

The k_{veg} for savannas was recalibrated after a first run of the model. We performed a qualitative comparison between our estimate of vapor flows from actual land cover and an estimate of present vapor flows in the global-water-use and hydrology model WATERGAP 2.1 developed by Döll and colleagues (29), which showed our data to be much lower from savannas than what was found in WATERGAP 2.1. In the final run of the model, we assumed a k_{veg} for savannas corresponding to the average value of k_{veg} for grassland and forest (0.25 for summer and 0.45 for winter months) (Table 1). This assumption seems valid because tree cover determines the distribution of savannas in the vegetation classification, placing them geographically between grasslands (<10% tree cover) and forests (>80% tree cover).

Results

The total global vapor flows for potential vegetation was estimated at 67,000 km³/yr. Fig. 1 shows the distribution of vapor flows, clearly illustrating the major contribution of the humid tropical regions to the total global flow and underscoring the importance of these regions for this aspect of Earth System functioning. The highest vapor flows are found in the Southeast Asian archipelago, which, when coupled with the high evaporation rates from the adjacent warm surface waters of the western Pacific Ocean and eastern Indian Ocean, shows why this region is so important for the functioning of the Earth System.

The areas where the conversion of forests to another land-cover type has led to significant changes in vapor flows are shown in Fig. 2. Aggregated globally, the net decrease of vapor flows due to deforestation is ≈3,000 km³/yr, which is 4% of the total global vapor flow from the land surface. However, the global total does not reveal significant regional differences. The main areas that have experienced decreases are Southeast Asia (par-

ENVIRONMENTAL SCIENCES

Fig. 1. Spatial distribution of annual water vapor flows (mm/yr) from potential vegetation, illustrating water vapor flows before human impacts. The figure illustrates the importance of vapor flows from the humid tropics. The total global vapor flow amounts to 67,000 km^3/yr.

ticularly the Philippine Islands, Sumatra, and Borneo), southwestern and central Africa, the arc of deforested areas around the edge of the Amazon basin, northern South America, and the temperate forest regions of the eastern United States and central and western Europe (Fig. 2).

The increases in vapor flows owing to irrigation are shown in Fig. 3. Aggregated globally, the net increase through irrigation was found to be ≈2,600 km^3/yr, which is consistent with previous global estimates that range from 1,800 to 2,500 km^3/yr (5, 6, 30–31). The only estimate based on the same data set of irrigation as our study, however, is more conservative (1,100 km^3/yr) (32). The authors of ref. 32 suggest a method of

modeling global irrigation requirements that separates rice from other cereals and builds on length of growing periods for different crops and in different regions. This is a more sophisticated method than ours. However, because our result is consistent with other estimates, we believe it to be appropriate for this first-cut global estimation.

With irrigation, there is, again, a large regional variation, the most prominent regions of irrigation clearly correlated with areas of intensive food production: southeastern China and, especially, the Indo-Gangetic Plain of the Indian subcontinent. Significant vapor flows from irrigation also occur in central Asia, the central and western United States, southern Europe, and north-central Chile.

Fig. 2. Spatial distribution of changes in vapor flows due to deforestation (mm/yr), based on the change in vapor flows between potential vegetation and actual vegetation in deforested areas. The total decrease in vapor flows is ≈3,000 km^3/yr.
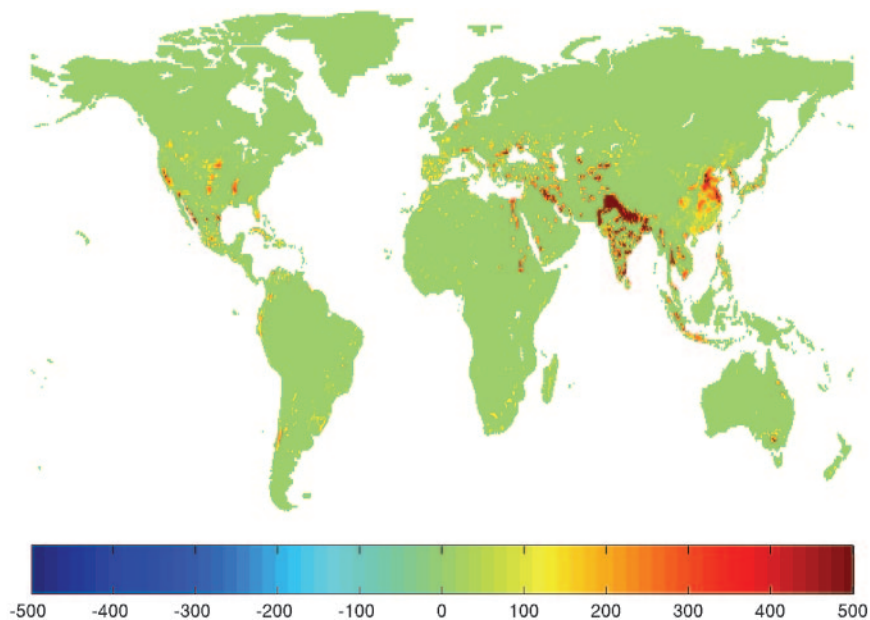
Fig. 3. Spatial distribution of changes in vapor flows due to irrigation (mm/yr), defined as the change in vapor flows when irrigation only is added to actual vegetation. The total increase in vapor flows amounts to 2,600 km^3/yr.

Discussion

Our results show that deforestation is as large a driving force as irrigation in the human alteration of global vapor flows. Thus, at the global aggregate level, there has not been a substantial net change in vapor flows. The decrease in vapor flows of 3,000 km^3/yr from deforestation is almost compensated for by increased vapor flows from irrigation of 2,600 km^3/yr. The combined effects of deforestation and irrigation have led to substantial redistribution of vapor flows at the global scale, as shown in Fig. 4.

Three different types of regional vapor-flow change can be seen: (*i*) regions with net loss of vapor flows from deforestation and no compensation from irrigation (e.g., around the Amazon Basin); (*ii*) regions with increased vapor flows due to irrigation (e.g., the western United States, where many of these irrigated regions are in semiarid zones and carried no dense forests originally); and (*iii*) regions where loss of vapor flow from deforestation is compensated for by increases from irrigation (e.g., northern China).

The total continental vapor flow for actual vegetation of 66,600 km^3/yr corresponds well with previous global estimates of water vapor flow that range from 61,000 to 72,500 km^3/yr (2, 33, 34). In Table 2, we compare our biome-specific vapor flow (mm/yr) with estimates from a review of field data on annual
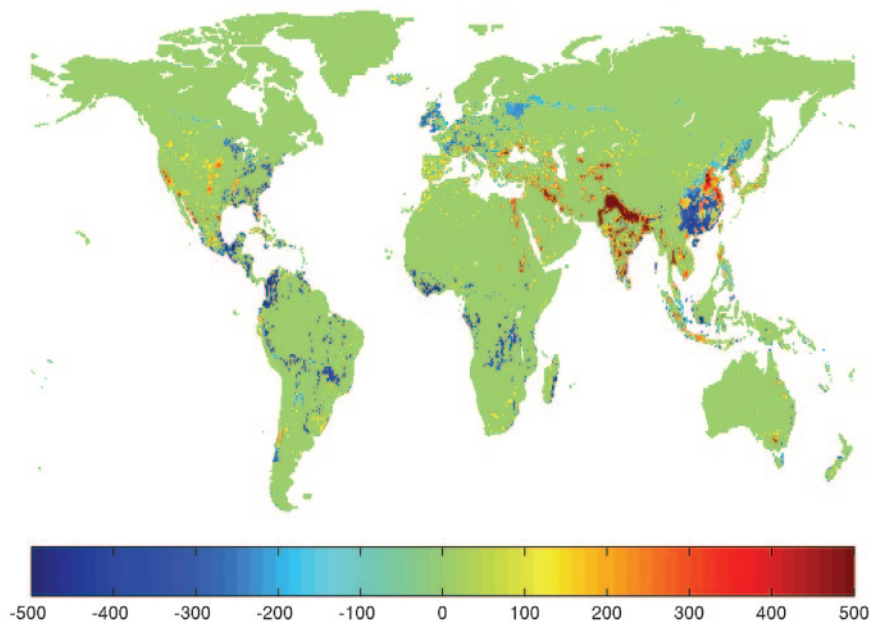

Fig. 4. Spatial distribution of net changes in vapor flows between potential vegetation and actual deforested and irrigated vegetation in mm/yr. The aggregated global change as compared with the potential vegetation is small (400 km^3/yr), but the map illustrates the large spatial redistribution of water vapor flows from the land surface at the global scale.

ENVIRONMENTAL
SCIENCES

Table 2. Comparison between the estimate of vapor flows from various biomes in the model of this article and field data from Rockström *et al.* (2)

| | Model data | | Field data | |
Biome	Vegetation type	Vapor flow, mm/yr	Vegetation type	Vapor flow, mm/yr
Forests/woodlands				
Tropical	Evergreen forest/woodland	1,146	Wet forest	1,245
	Deciduous forest/woodland	795	Forest, dry/deciduous/seasonal	792
Temperate	Needleleaf evergreen forest/woodland	510	Predominantly coniferous forest	487
	Broadleaf evergreen forest/woodland	592	Predominantly deciduous forest	729
	Deciduous forest/woodland	553		
Boreal	Evergreen forest/woodland	339	Taiga	401
	Deciduous forest/woodland	293		
	Evergreen/deciduous mixed forest/woodland	313		
Savanna*	Savanna	556	Savanna/woodland, dry	882
			Wet savanna	1,267
			Woodland/woody savanna	416
Grasslands/shrublands	Grassland/steppe	258	Cool grassland	410
	Marginal cropland used for grazing	431		
	Dense shrubland	280	Dry shrubland	270
	Open shrubland	196		

*Savanna in this estimate is based on both tropical and temperate savannas/woodlands, whereas the estimate by Rockström *et al.* (2) includes only tropical savannas.

vapor flows in various biomes (2). The comparison reflects a high level of agreement between the field data and our estimate.

The global pattern of vapor flows from the land surface to the atmosphere will change further over the next 50 yr to meet the food requirements of a population of eight to nine billion and to reduce today's malnourishment. The need to nearly double vapor flows associated with food production (3, 4) implies significant regional changes in vapor flows in several parts of the world, with likely global-scale impacts on the functioning of the Earth System.

Much interest has focused on the Amazon Basin. Currently, about 15% of the Brazilian Amazon has been deforested and converted to agricultural uses, with concomitant decreases in vapor flows (Fig. 2). Model projections suggest that there is a critical threshold beyond which the reduction in rainfall due to reduced vapor flows leads to dieback of the forest, thus forming a positive feedback loop that hastens the conversion of rainforest to savanna or grassland (35). Conversion of the Amazon rainforest would obviously have large impacts on regional vapor flows with possible global consequences for climate, but projections of future land-cover change in the Amazon Basin are not consistent, with some projections showing that much of the rainforest will still remain by the end of this century (36).

More likely and more immediate, however, are changes in the pattern of vapor flows around the Indian Ocean basin. South Asia and sub-Saharan Africa are two regions with an acute need to increase food production (37). Irrigation is widespread in South Asia, and vapor flows have already increased substantially (Fig. 3). Given the looming water scarcity in the region, future increases in food availability will likely come from increased production efficiency and from food trade (i.e., virtual water trade). In sub-Saharan Africa, on the other hand, increased food production will most likely come from further expansion of agricultural land through deforestation (36), causing a net decrease in vapor flows. Coupled with the substantial changes in vapor flows that have already occurred in Asia (Fig. 2), the deforestation of sub-Saharan Africa would create a ring of highly modified terrestrial vapor flows around the Indian Ocean basin, a key component of the Asian monsoon system. Given the apparent

sensitivity of the Asian monsoon system to land-cover change (19), further modification of vapor flows in the lands around the Indian Ocean basin will increase the risk for changes in the behavior of the Asian monsoon system, raising the possibility that the need to increase food production in one region (sub-Saharan Africa) may affect the capability to increase food production in another (South Asia).

In terms of the functioning of Earth System as a whole, our results also raise important questions related to the relative role of land-use and climate change in altering vapor flows. For example, we know that the vapor flows from the oceans amount to ≈80–85% of the total vapor flow from the Earth's surface. It has been estimated that climatic changes in the last four decades have changed vapor flows over the oceans by 0.2–0.5 mm/day, with both increases and decreases depending on location and season (38). No consistent estimate exists of climatic-change effects on vapor flows from terrestrial areas. Some estimates indicate a decrease in pan evaporation in some regions despite a temperature increase over the past 50 yr (39), whereas others show increased evaporation from many land areas over the past 30 yr due to increased temperature (40). The relative magnitude of changes in water vapor flow due to land-use change compared with those due to climatic change thus remains unknown and needs to be explored in further work.

Our estimate illustrates the need to increase the understanding of direct human alteration of water vapor flows from the land surface on atmospheric circulation by including the impact of land-use change in global climate models. In particular, the results show that the effects of irrigation on water vapor flows are equally as important as deforestation in describing the climatic effects of human modification of the land surface.

1. Postel, S. L. (2003) *Nat. Resour. Forum* **27,** 89–98.
2. Rockström, J., Gordon, L., Folke, C., Falkenmark, M. & Engwall, M. L. (1999) *Conserv. Ecol.* **3**. Available at www.consecol.org/vol3/iss2/art5.
3. Postel, S. L. (1998) *Bioscience* **48,** 629–637.
4. Rockström, J. (2003) *Philos. Trans. Roy. Soc. London B*, **358** 1997–2009.
5. Postel, S. L., Daily, G. C. & Ehrlich, P. R. (1996) *Science* **271,** 785–788.
6. Gleick, P. H. (1993) *Water in Crisis: A Guide to the World's Fresh Water Resources* (Oxford Univ. Press, New York).
7. Dynesius, M. & Nilsson, C. (1994) *Science* **266,** 753–762.
8. Vörösmarty, C. J., Sharma, K. P., Fekete, B. M., Copeland, A. H., Holden, J., Marble, J. & Lough, J. A. (1997) *Ambio* **26,** 210–219.
9. Rosenberg, D. M., McCully, P. & Pringle, C. (2000) *Bioscience* **50,** 746–751.
10. Smakhtin, V., Revenga, C. & Döll, P. (2004) *Taking into Account Environmental Water Requirements in Global-Scale Water Resources Assessments* (Comprehensive Assessment, Colombo, Sri Lanka), Comprehensive Assessment Research Report 2.
11. Kabat, P., Claussen, M., Dirmeyer, P. A., Gash, J. H. C., Bravo de Guenni, L., Meybeck, M., Pielke, R. A., Sr., Vörösmarty, C. J., Hutjes, R. W. A. & Lütkemeier, S. (2004) *Vegetation, Water, Humans and Climate: A New Perspective on an Interactive System* (Springer, Berlin).
12. Fu, C. (2003) *Glob. Planet. Change* **37,** 219–229.
13. Gordon, L., Dunlop, M. & Foran, B. (2003) *Philos. Trans. Roy. Soc. London B* **358,** 1973–1984.
14. Nemani, R. R., Running, S. W., Pielke, R. A. & Chase, T. N. (1996) *J. Geophys. Res.* **101,** 7157–7162.
15. Marland, G., Pielke, R. A., Sr., Apps, M., Avissar, R., Betts, R. A., Davis, K. J., Frumhoff, P. C., Jackson, S. T., Joyce, L., Kauppi, P., *et al.* (2003) *Climate Policy* **3,** 149–157.
16. Baron, J. S., Hartman, M. D., Kittel, T. G. F., Band, L. E., Ojima, D. S. & Lammers, R. B. (1998) *Ecol. Appl.* **8,** 1037–1051.
17. Chase, T. N., Pielke, R. A., Kittel, T. G. F., Baron, J. S. & Stohlgren, T. J. (1999) *J. Geophys. Res. Atmos.* **104,** 16673–16690.
18. Pielke, R. A., Lee, T. J., Copeland, J. H., Eastman, J. L., Ziegler, C. L. & Finley, C. A. (1997) *Ecol. Appl.* **7,** 3–21.
19. Fu, C. & Yuan, H. (1994) *Chin. Sci. Bull.* **45,** 1199–1203.
20. Zheng, X. & Eltahir, E. A. B. (1998) *J. Climate* **11,** 2078–2096.
21. Bosch, J. M. & Hewlett, J. D. (1982) *J. Hydrol.* **55,** 3–23.
22. Ramankutty, N. & Foley, J. A. (1999) *Glob. Biogeochem. Cycles* **13,** 997–1027.
23. Goldewijk, K. K. (2001) *Glob. Biogeochem. Cycles* **15,** 417–433.
24. Willmott, C. J. & Matsuura, K. (1998) *Global Air Temperature and Precipitation: Regridded Monthly and Annual Climatologies* (Center for Climatic Research, University of Delaware, Newark), Version 2.01.
25. Döll, P. & Siebert, S. (1999) *A Digital Global Map of Irrigated Areas* (Center for Environmental Systems Research, Kassel, Germany), Report A9901.
26. Holland, H. D. (1978) *The Chemistry of the Atmosphere and Oceans* (Wiley, New York).
27. Federer, C. A., Vörösmarty, C. & Fekete, B. (1996) *Water Resour. Res.* **32,** 2315–2321.
28. Dudhia, J., Gill, D., Guo, Y.-R., Hansen, D., Manning, K. & Wang, W. (1999) *PSU/NCAR Mesoscale Modeling System Tutorial Class Notes and Users' Guide: MM5 Modeling System Version 2* (Mesoscale and Microscale Meteorology Division, National Center for Atmospheric Research, Boulder, CO).
29. Döll, P., Kaspar, F. & Lehner, B. (2003) *J. Hydrol.* **270,** 105–134.
30. L'vovich, M. I. & White, G. F. (1990) in *The Earth as Transformed by Human Action: Global and Regional Changes in the Biosphere Over the Past 300 Years*, eds. Turner, B. L., Clark, W. C. & Kates, W. C. (Cambridge Univ. Press, Cambridge, U.K.).
31. Shiklomanov, I. A. (2000) *Water Int.* **25,** 11–32.
32. Döll, P. & Siebert, S. (2002) *Water Resour. Res.* **38,** 10.1029/2001WR000355.
33. Baumgartner, A. & Reichel, E. (1975) *The World Water Balance* (Elsevier, New York).
34. L'vovich, M. I. (1979) *World Water Resources and Their Future* (LithoCrafters Chelsea, U.K.).
35. Oyama, M. D. & Nobre, C. A. (2003) *Geophys. Res. Lett.* **30,** 2199–2203.
36. de Vries, H. J. M., Bollen, J., Bouwman, L., den Elzen, M. G. J., Janssen, M. & Kreilemann, E. (2000) *Technol. Forecast Soc.* **63,** 137–174.
37. Food and Agriculture Organization (2002) *The State of Food and Agriculture. The State of Agriculture and Global Public Goods Ten Years After the Earth Summit* (Food and Agriculture Organization of the United Nations, Rome).
38. Intergovernmental Panel on Climate Change (IPCC) (1995) *Climate Change 1995: The Science of Climate Change*. Contribution of the Working Group 1 to the Second Assessment of the IPCC, eds. Houghton, J. T., Meira Filho, L. G., Callender, B. A., Harris, N., Kattenberg, A. & Maskell, K. (Cambridge Univ. Press, Cambridge, U.K.).
39. Ohmura, A. & Wild, M. (2002) *Science* **298,** 1345–1346.
40. Dai, A., Trenberth, K. E. & Qian, T. (2004) *J. Hydrometeorol.* **5,** 1117–1130.

ENVIRONMENTAL SCIENCES